Shahrood University of Technology

Journal of Mining and Environment (JME)

Journal homepage: www.jme.shahroodut.ac.ir

Iranian Society of Mining Engineering (IRSME)

Strength and Durability of Cement Based CLSM Developed using Iron Mine Overburden

Tulika Gupta[1], Mahasakti Mahamaya[1], and Shamshad Alam[2]*

1. Department of Civil Engineering, School of Engineering, OP Jindal University, Raigarh, India
2. Civil and Architectural Engineering Department, College of Engineering and Computer Science, Jazan University, Jazan, Saudi Arabia

Article Info

Received 19 August 2025
Received in Revised form 26 September 2025
Accepted 15 November 2025
Published online 15 November 2025

DOI: 10.22044/jme.2025.16705.3277

Keywords

Flowability
Bleeding
Strength
Durability

Abstract

The dumping of mining waste occupies extensive areas of land and poses environmental hazards, including heavy metal leaching, dust pollution, and slope failure. Iron mine overburden (MO), a byproduct of iron mining, exacerbates these issues when dumped. To address the challenges of storing MO, it was combined with fly ash and cement to develop controlled low-strength material (CLSM). Initially, the raw materials were examined for their physical, chemical, and mineralogical properties. Subsequently, 24 different CLSM mixtures were prepared by varying cement, fly ash, MO, and water-to-binder ratios. The fresh mixes were tested for flowability, bleeding, and fresh density, while the hardened properties, including density, unconfined compressive strength (UCS), and durability, were also evaluated. Results showed that all CLSM mixes were highly flowable, with flow diameters exceeding 150 mm, and some exhibited self-leveling behavior. The 28-day compressive strength ranged from 0.52 MPa to 4.28 MPa, with a few mixes being soft enough for manual excavation. Durability tests indicated that approximately 60% of the mass remained intact after eight wet-dry cycles, demonstrating good resistance to erosion. This study highlights the potential for utilizing mining waste in sustainable construction materials.

1. Introduction

Mine overburden is a waste material that is available above the mineral deposit. In open-cast mining, the overburden must be removed to access the mineral deposits. The mine overburden mostly consists of rock and soil with varying particle sizes. Storage of mine overburden poses environmental challenges due to heavy metal leaching [1] and is also susceptible to slope instability issues [2], which further exacerbate these problems. Several researchers have examined the impact of mine overburden dumping on slope stability [3, 4]. Various techniques, such as biogeochemical methods and adsorption methods, have been employed to mitigate environmental problems caused by the storage of mine overburden [5–7]. To reduce pollution from sulfur and toxic metals, segregating materials before dumping has been identified as an effective approach [8]. However, these safe dumping techniques for mine overburden are unable to resolve the storage problem, which consumes large areas of land. To address this, several researchers have explored the potential applications of mine overburden in the construction industry. A mixture of mine overburden, fly ash, and cement (4–7%) has been found to be an effective pavement material [9]. Coal mine overburden can also be used for underground mine backfilling, offering a sustainable solution [10]. With an unconfined compressive strength (UCS) ranging from 0.3 MPa to 8.3 MPa [11], controlled low-strength material (CLSM) meets the strength requirements for geotechnical applications. Additionally, CLSM offers several advantages over conventional compacted soil, including self-leveling and self-compacting properties that reduce heavy equipment costs, accelerate construction, and enable use in confined spaces [12]. These benefits

Corresponding author: shalam@jazanu.edu.sa (S. Alam)

have increased interest in developing CLSM from industrial waste for applications such as grouting, backfilling, and pavement bases [13–15]. Various waste materials, including fly ash, slag, red mud, and mine waste, have been successfully incorporated into CLSM [16–22]. Although iron mine overburden has been studied for use in construction industries, its potential for CLSM development remains unexplored. Conversely, the heavy reliance on natural soil for backfilling and embankment construction leads to resource depletion. To address concerns related to mine overburden handling and natural resource conservation, this research investigates the potential utilization of iron mine overburden. The study aims to develop CLSM using iron mine overburden in combination with fly ash and cement. Key properties such as flowability, bleeding, density, UCS, water absorption, and durability are evaluated. Self-leveling behavior was assessed via the relative flow area (RFA), while excavation feasibility was determined through 28-day UCS and density measurements. By incorporating iron mine overburden into CLSM, this research seeks to manage waste effectively while promoting sustainable construction practices.

2. Materials and Methodology

The iron mine overburden (MO) used in the present research was obtained from the TRB iron ore mine situated in the Tensa valley in the Sundargarh district of Odisha, India. The fly ash was collected from Jindal Power Limited, Raigarh, India. For the development of CLSM, iron mine overburden was used as aggregate, whereas the fly ash with ordinary Portland cement of grade 53 (OPC 53) was used as the binder material. The iron mine overburden and fly ash were dried in an electric oven at 100°C to 105°C for 24 hours before being used in the CLSM. Initially, the waste material was characterized considering its morphology, surface chemistry, mineralogy, and physical properties. The morphology and surface chemistry were analyzed using a scanning electron microscope (SEM) equipped with an energy-dispersive X-ray (EDX) microanalyzer. Mineralogical composition was examined through X-ray diffraction (XRD) analysis with CuKα radiation, covering a 2θ range of 10° to 70° at a scanning rate of 4°/min. Figure 1 presents SEM images of iron mine overburden and fly ash at a 100 µm scale. The fly ash (Figure 1a) is predominantly composed of spherical particles, likely cenospheres, while MO (Figure 1b) contains solid, irregular-shaped particles in platelike structures. Similar observations for fly ash particles [23–25] and coal mine overburden [5, 26] have been reported by earlier researchers.

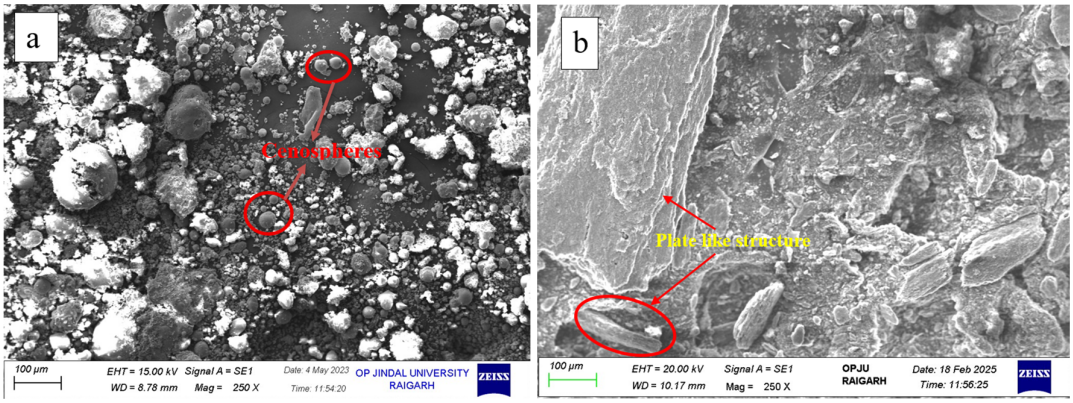

Figure 1. SEM image of (a) fly ash and (b) iron mine overburden

The surface chemistry of both materials, such as fly ash and iron mine overburden, was analyzed across a specified area, with the results summarized in Table 1, while the corresponding EDX spectra are displayed in Figure 2a and Figure 2b for fly ash and iron mine overburden, respectively. According to Table 1, the fly ash surface consists of 52.2% oxygen along with 26.8% silica and 17.9% aluminum (Table 1), which is very similar to the results observed by earlier researchers [23, 25], and can also be observed with an intense peak in Figure 2a.

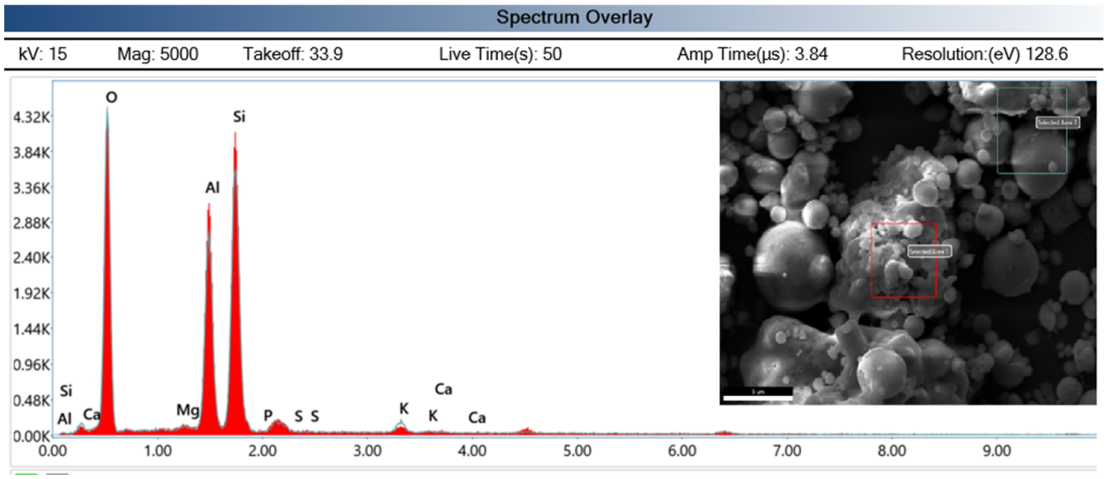

Figure 2a. EDX of fly ash

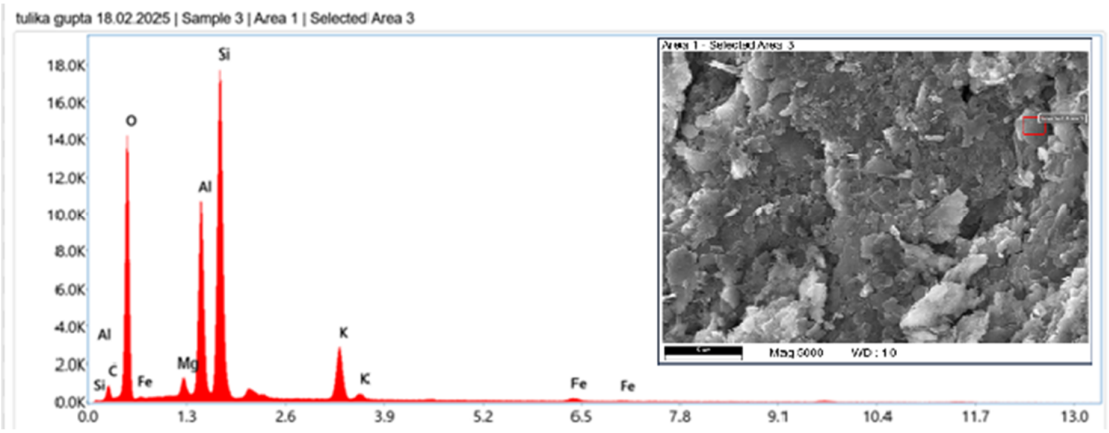

Figure 2b. EDX of iron mine overburden

The EDX result of iron mine overburden reflects that oxygen (51%) is the most prevalent element at the surface of the iron mine overburden, followed by silica (17.4%), carbon (14.7%), and aluminum (10.3%). Additionally, minor amounts of potassium (4.7%), magnesium (1.3%), and iron (0.6%) were also detected, which is further supported by the EDX micrograph in Figure 3a.

Furthermore, the mineralogy of the iron mine overburden and fly ash is presented in Figure 3 in the form of an XRD graph. An intense peak of silica can be observed in fly ash, whereas a strong peak of muscovite, a mineral containing silica, iron, and aluminum, can be observed in the iron mine overburden. The strong peak of silica compound confirms the abundance of silica in these materials, as also observed in surface chemistry (Table 1).

Table 1. Surface chemistry of MO and fly ash

Element	MO (% weight)	Fly ash (% weight)
C	14.7	-
O	51	52.2
Mg	1.3	0.7
Al	10.3	17.9
Si	17.4	26.8
Ca	-	0.3
Fe	0.6	-
P	-	0.6
S	-	0.5
K	4.7	1.2

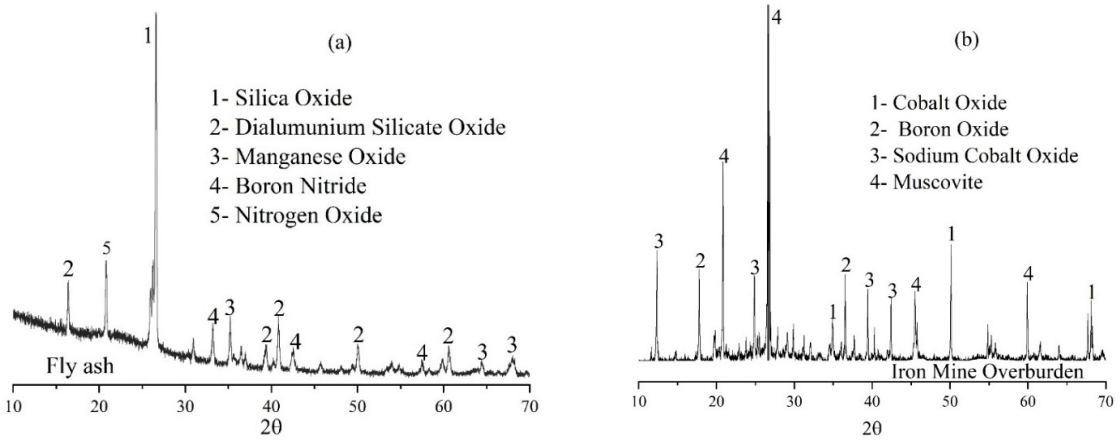

(a) **(b)**

Figure 3. XRD graph of (a) fly ash, and (b) iron mine overburden

In fly ash, aluminum exists as aluminum silicate, while in iron mine overburden, it is found in the form of the mineral muscovite. The XRD analysis (Figure 3) of both materials verifies their mineralogical composition, revealing distinct chemical compounds on the surfaces of iron mine tailings and fly ash (Table 1). The specific gravity of the materials was measured via the water displacement method using a pycnometer [27]. Particle size distribution analysis, performed using mechanical sieving [28], is illustrated in Figure 4. The results indicate that the iron mine overburden is a poorly graded material with approximately 9.05% fine fraction, while nearly 99.95% of fly ash particles are finer than 0.075 mm. Furthermore, MO contains more than 50% gravel-sized particles with 9.05% fine. The fine particles of MO showed a liquid limit of 31% and a plasticity index of 26.63%, and can be classified as poorly graded gravel with silty sand [29]. Additionally, fly ash consists of 37.81% of particles in the 72.24–75 μm range, with 62.14% being smaller than 72.24 μm (Figure 4). Table 2 summarizes all the physical properties of the raw materials.

To assess the mechanical properties, the iron mine overburden (MO) and fly ash were combined in varying ratios along with cement and water to develop controlled low-strength material (CLSM) samples. Since flowability is a fundamental requirement for CLSM [30, 31], 24 different mixes were prepared by adjusting the proportions of cement, fly ash, MO, and the water-to-binder (W/B) ratio to meet this criterion. During mix design, the cement content was varied as 9%, 11%, 13%, and 15% of the total dry weight of the mixture. The variation of cement was selected based on prior research, which recommends a cement content ranging from 9% to 15% [32–35]. A symbol "Wn" has been used for different values of the water-to-binder ratio, where "n" varies from 1 to 12 as presented in Table 3. The Mix ID for each sample, reflecting different compositions of materials and water-to-binder ratios, is provided in Table 4.

Table 2. Physical properties of raw materials

Parameters	Values	
	MO	Fly ash
Specific gravity	1.77	2.26
Crushing value	43.89	-
Abrasion value	45.81	-
Coefficient of curvature	68.4	0.64
Coefficient of uniformity	0.54	7.01

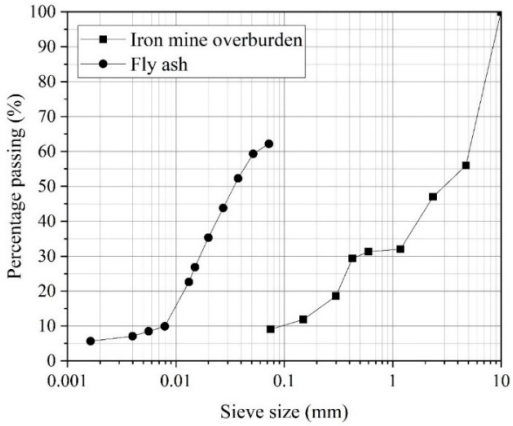

Figure 4. Particle size distribution of iron mine overburden and fly ash

Table 3. Table showing the symbol corresponding to different W/B ratio

Symbol	W1	W2	W3	W4	W5	W6	W7	W8	W9	W10	W11	W12
W/B	0.525	0.55	0.575	0.6	0.625	0.65	0.675	0.7	0.725	0.75	0.775	0.8

Table 4. Mix ID corresponding to different percentage of cement, fly ash and MO

Mix ID	W/B	Binder (%)		Aggregate (%)
		Cement	Fly ash	MO
M1W6	0.65	9%	36%	55%
M1W7	0.675			
M1W8	0.7			
M1W9	0.725			
M2W1	0.525	11%	55%	38%
M2W2	0.55			
M2W3	0.575			
M2W4	0.6			
M3W4	0.6	11%	38%	55%
M3W5	0.625			
M3W6	0.65			
M3W7	0.675			
M4W1	0.525	13%	55%	32%
M4W2	0.55			
M4W3	0.575			
M4W4	0.6			
M5W9	0.725	15%	32%	53%
M5W10	0.75			
M5W11	0.775			
M5W12	0.8			
M6W1	0.525	15%	53%	32%
M6W2	0.55			
M6W3	0.575			
M6W4	0.6			

In Table 3, "M" denotes the mix designation, indicating varying proportions of cement, MO, and fly ash. The symbol "W" represents the water-to-binder ratio ranging from 0.525 to 0.8 and was adjusted according to the flowability requirements of CLSM. For each flowability test, a 2 kg dry mixture was prepared with different percentages of cement, fly ash, and MO. Later, the slurry was prepared by adding water to the dry mixture at different water-to-binder ratios. Following slurry preparation, flowability testing was performed according to ASTM D6103 standards [36]. For this purpose, a 3-inch diameter PVC pipe measuring 6 inches in length was used, as shown in Figure 5. The PVC pipe was placed on a level acrylic surface and filled with CLSM slurry. The pipe was then carefully lifted to allow the material to spread over the surface (Figure 5). Further, the flow diameter (D) was measured using a metallic tape, and the measured diameter was used to calculate the relative flow area (RFA) using Equation 1 [37]. The relative flow area is important for understanding the leveling consistency of the CLSM. A higher RFA value (> 5) indicates that the CLSM has self-leveling properties [38].

$$RAF = \left({}^{D}/_{100}\right)^{2} - 1 \quad (1)$$

Figure 5. Flowability test setup

Bleeding is a critical phenomenon in CLSM that leads to the separation of water from the solid constituents. In this study, bleeding behavior was evaluated following ASTM C1610 standards [39]. Initially, the CLSM slurry was poured into a 1000 ml graduated measuring cylinder and left undisturbed for 3 hours to allow material settlement. Later, the volume of separated water that accumulated at the surface was measured (Figure 6). Bleeding was then calculated as the percentage of water accumulated at the surface relative to the total initial volume of the CLSM slurry.

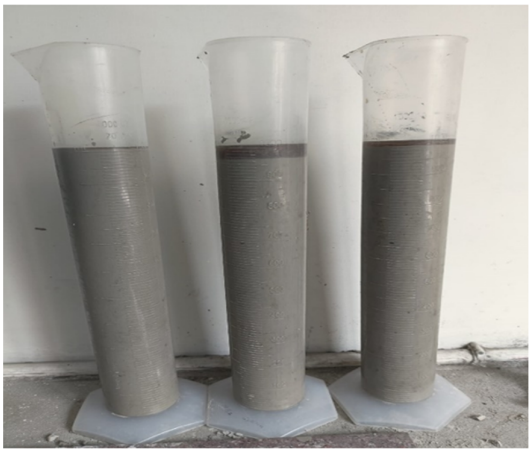

Figure 6. Bleeding test setup

Furthermore, the density of the CLSM was evaluated in both the fresh and hardened states. Fresh density measurements followed ASTM D6023 [40] guidelines, while hardened density was determined by measuring the mass and volume of specimens after curing periods of 7, 14, 28, and 60 days. Unconfined compressive strength (UCS) testing was performed according to ASTM [41] standards using cylindrical specimens (53 mm diameter × 106 mm height). The UCS was evaluated after curing periods of 7, 14, 28, and 60 days, with triplicate samples tested for reliability. Additionally, the excavability characteristic of CLSM was quantified through the removability modulus (RE). The removability modulus was calculated using on-site density and 28-day UCS values according to Equation 2 [18]. A removability modulus less than 1 indicates that the CLSM can be manually excavated.

$$RE = \frac{0.618 \times w^{1.5} \times C^{0.5}}{10^6} \leq 1 \qquad (2)$$

Where are:

RE – removability modulus,

w – on-site density in kg/m^3,

C – 28 days compressive strength in kPa.

3. Results and Discussion

3.1. Flowability and Bleeding

The characteristics of fresh CLSM were evaluated based on flowability, bleeding, and fresh density. Flowability is a key factor, with a minimum requirement of 150 mm for CLSM [31]. As shown in Figure 7, all the specimens developed in this study exceeded 150 mm in flowability, and this value increased further with a higher water-to-binder ratio. Earlier researchers have also achieved the required minimum flowability at these water-to-binder ratios for fly ash-based CLSM [22, 26]. Besides the water-to-binder ratio, flowability was found to be controlled by the percentage of fly ash. It was observed that, for a similar percentage of cement, CLSM containing a higher percentage of fly ash requires a lower water-to-binder ratio to achieve the desired flowability. This may be due to the spherical shape of fly ash particles, which provides a ball-bearing effect and enhances flowability [42, 43]. Conversely, due to the porous structure of mine overburden, CLSM with a higher percentage of mine overburden requires a higher water-to-binder ratio to attain the minimum flowability, as seen in the cases of M2W4, M3W4, M2W1, and M4W1. Subsequently, the segregation of solid particles was studied based on bleeding behavior. The results are presented as percentages of segregated water relative to the total volume of CLSM (Figure 7). The data reveal that for a water-to-binder ratio up to 0.8, the 3-hour bleeding remains below the 5% threshold limit [16, 44, 45].

Moreover, the self-leveling behavior of CLSM [12, 46] was examined by determining the relative flow area using Equation (1), and the results are shown in Figure 8. Despite meeting the flowability and bleeding criteria (Figure 7), most specimens were found not to be self-leveling, except for the M6W4 specimen (Figure 8), which exhibits a relative flow area above 5 [37]. The self-leveling property can be improved by increasing the water-to-binder ratio; however, bleeding at the elevated water-to-binder ratio must remain within permissible limits (<5%).

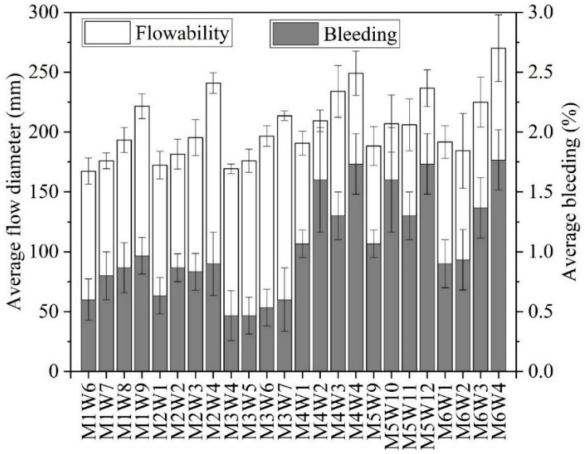

Figure 7. Average flowability and bleeding of different specimen

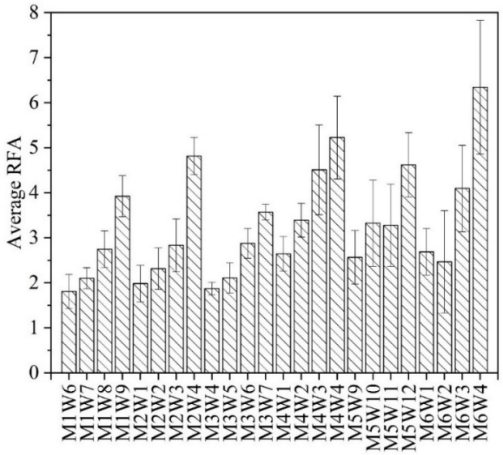

Figure 8. Relative flow area calculated based on flowability

3.2. Density and Water Absorption

As per the standards [30, 47], the density of fresh CLSM must fall within 1360–2023 kg/m³, whereas hardened CLSM should have a lower density compared to its fresh density. In this research, the density of fresh and hardened CLSM was calculated based on the mass and volume of the specimen. The results for the fresh and hardened density of CLSM are presented in Figure 9 and Figure 10, respectively. The fresh density of all CLSM specimens developed in this research was found to be within the recommended range of 1360–2023 kg/m³ (Figure 9). The density of hardened CLSM varied between 1226.80 kg/m³ and 1816.82 kg/m³ (Figure 10), which is below their corresponding fresh density. The reduction in the hardened density of CLSM is due to decreases in water content and increases in air content within the specimen [19]. Based on the density criteria, the developed material can be classified as CLSM. Furthermore, it was observed that the change in density with curing time does not follow a specific decreasing or increasing trend. To understand this unpredictable behavior, further in-depth research is required in this area.

Additionally, the water absorption characteristics of various CLSM samples were assessed after 7, 14, 28, and 60 days of curing. The average value of the percentage water absorption has been presented in Figure 11. The findings indicate that the CLSM mixtures exhibited higher percentages of water absorption, varying from 1.19% to 28.24%. A similar water absorption value was observed for the CLSM developed from fly ash and bottom ash [48]. It was further observed that an increase in curing time increases the water absorption. This increase in water absorption is due to the dissolution of the pozzolanic materials, which causes the formation of micropores, resulting in the water movement through capillary action [49]. It was also observed that an increase in the percentage of fly ash lowers the water absorption due to the formation of C-S-H gel, which fills the micropores and prevents the capillary rise of water [50, 51].

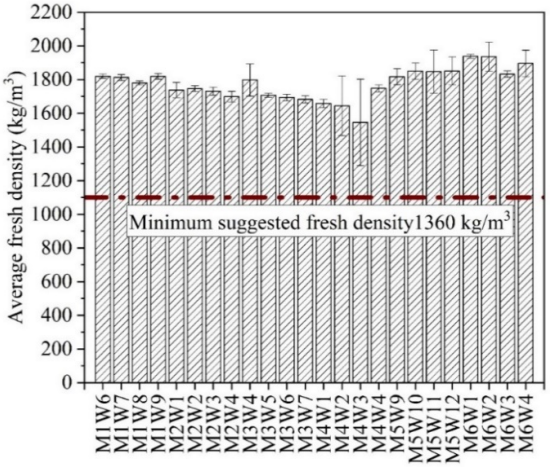

Figure 9. Average fresh density of different CLSM specimen

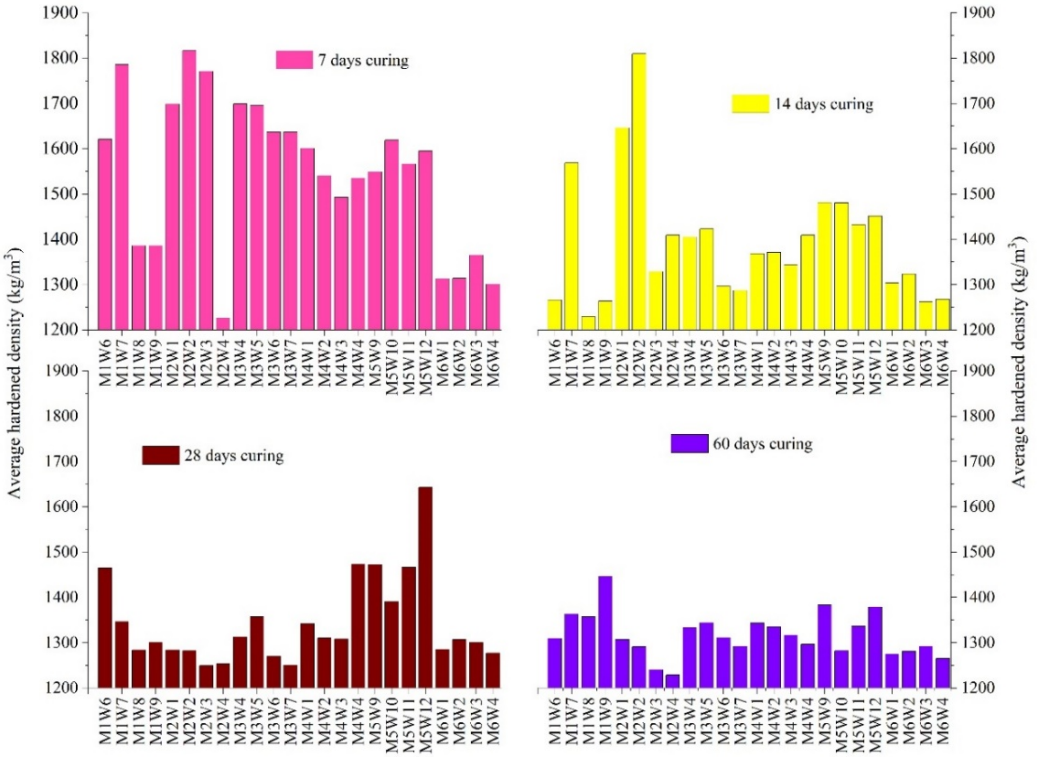

Figure 10. Average hardened density of different CLSM specimen

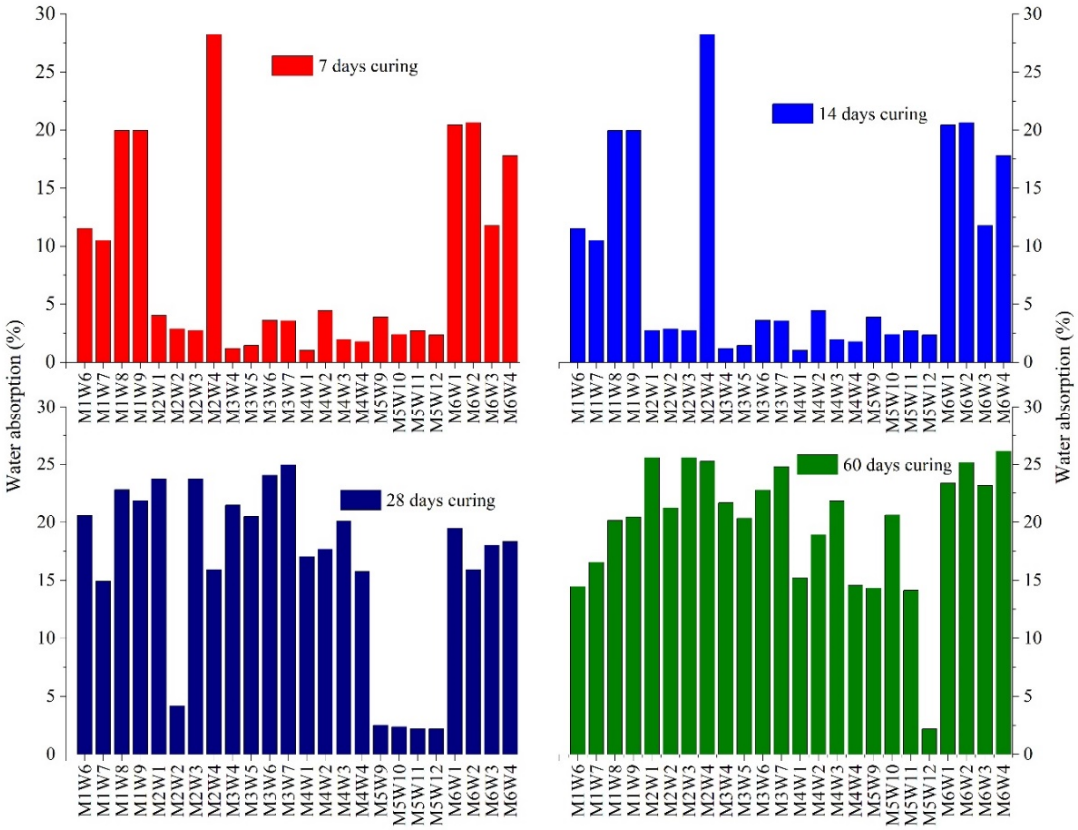

Figure 11. Water absorption of different CLSM specimen

3.3. Unconfined compressive strength (UCS)

The unconfined compressive strength (UCS) of the CLSM was tested after 7, 14, 28, and 60 days of curing, and the results are depicted in Figures 12–15. It was observed that increasing the percentage of fly ash enhances the UCS, whereas an increase in the water-to-binder ratio reduces the UCS value for most specimens. The lower UCS of specimens with higher water-to-binder ratios is due to decreased density after a specific curing period. Simultaneously, UCS development over time indicates significant variability in strength gain. While previous studies on CLSM with less porous materials reported an increase in UCS with curing time [13, 18, 52, 53], irregularities have also been noted for CLSM containing coal mine overburden [26, 49] and coal washery waste [23]. These fluctuations are likely attributable to the high porosity and low crushing strength of the iron mine overburden particles used in the mix. Notably, this research represents the first investigation into iron mine overburden-based CLSM. Therefore, further detailed studies are necessary to fully understand its mechanical properties and ensure its reliability for field applications. Future work should also focus on optimizing mix designs and curing conditions to mitigate these variations and improve the material's practicality for construction use.

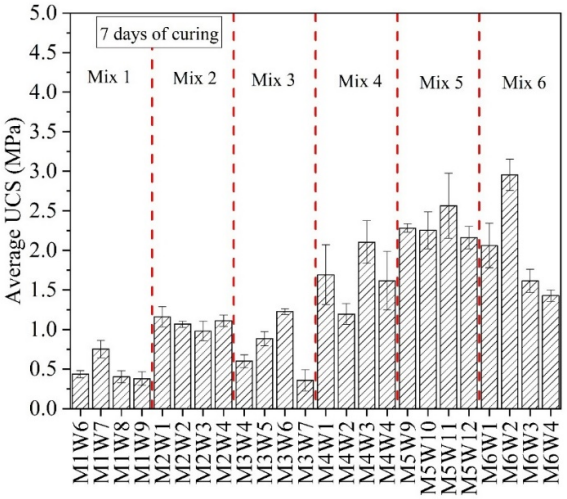

Figure 12. Average UCS different CLSM specimen after 7 days of curing

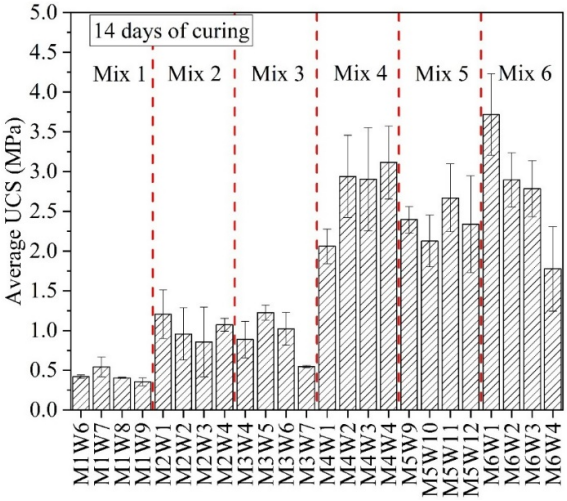

Figure 13. Average UCS different CLSM specimen after 14 days of curing

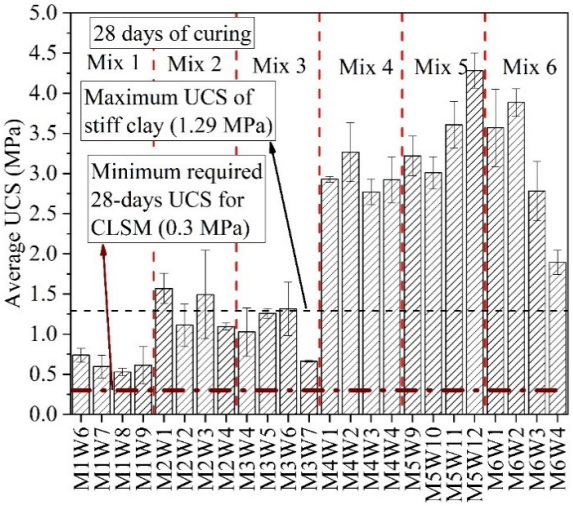

Figure 14. Average UCS different CLSM specimen after 28 days of curing

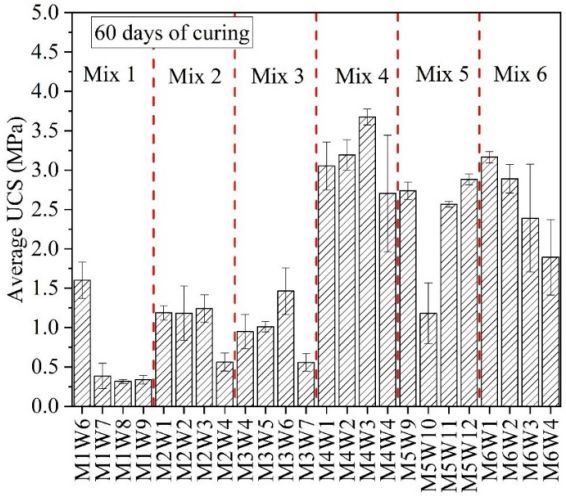

Figure 15. Average UCS different CLSM specimen after 60 days of curing

The 28-day unconfined compressive strength (UCS) of all the CLSM specimens ranged from 0.52 MPa to 4.28 MPa, as shown in Figure 14. The observed UCS values are well within the established CLSM range of 0.3–8.3 MPa [35, 54]. It is further observed that the UCS of all specimens of mixes M1 and M3, along with M2W2 and M2W4, varies between 0.392 MPa and 1.29 MPa, which is characteristic of stiff clay [55, 56]. Other mixtures exhibit superior strength to stiff clay, making them suitable for various engineering applications, including pavement bases, bridge abutments, retaining wall backfills, and thermal grouting, owing to their self-leveling and flow characteristics as reported in previous studies [13, 14, 47]. Additionally, since CLSM must be easily excavatable, their excavatability was assessed using 28-day UCS values and in-situ density according to Equation (2). The resulting excavatability characteristics of various CLSM mixtures are illustrated in Figure 16 in terms of removability modulus values. It is observed that all specimens of Mix M1, along with M2W2, M2W4, M3W4, and M3W7, are easy to excavate manually, with removability modulus values less than 1. However, the excavatability of all specimens of Mix M4, M5, and M6 is significantly higher than 1, rendering them non-manually excavatable. Furthermore, it can be concluded that all specimens of mixes M1, M2W2, M2W4, M3W4, M3W5, and M3W7, which have UCS values similar to stiff clay and removability modulus below 1, can be used as substitutes for clay in geotechnical structures.

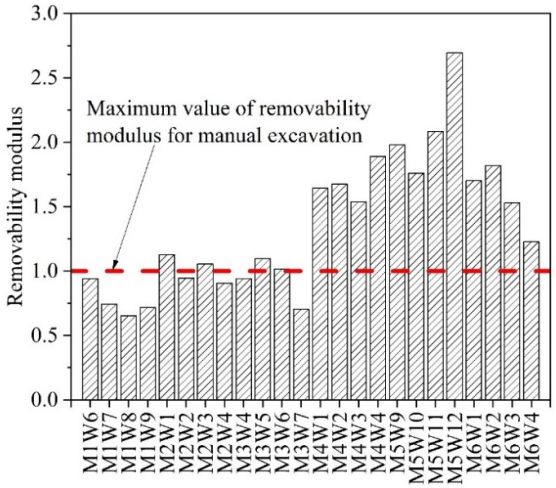

Figure 16. Excavatability of different mix proportion based on 28 days UCS

3.4. Durability

The stability of the soil is significantly affected by alternating wetting-drying cycles, which ultimately lead to increased mass loss. The expansion and contraction of the soil due to wet-dry cycles weaken its structure and enhance erosion. Understanding this phenomenon is important for assessing the long-term stability of geostructures. Therefore, this research studied the durability of the developed CLSM in terms of mass loss after different numbers of wet-dry cycles [57]. In the present study, one sample from each of Mix M1, Mix M2, Mix M3, Mix M4, Mix M5, and Mix M6 was selected for the durability test. Along with a typical photograph of a sample, Figure 17 shows the percentage mass loss of different specimens after various numbers of wet-dry cycles. It was observed that the mass loss increases and, in some cases, the specimen collapses with the increase in wet-dry cycles (Figure 17). The collapse of the specimen is represented as 100% mass loss in Figure 17. It was found that specimen M3W4 collapsed during the 9th cycle, specimen M2W1 collapsed during the 11th cycle, and specimen M6W1 collapsed during the 12th cycle. Additionally, specimens M1W6 and M4W1 also exhibited significant mass loss during the 12th cycle. Overall, all specimens showed substantial mass loss during the 12th cycle, except for specimen M5W9, which retained nearly 40% of its mass even after the 12th cycle (Figure 17). Furthermore, it can be noted that up to the 8th cycle, all specimens retained approximately 60% of their mass, indicating good performance.

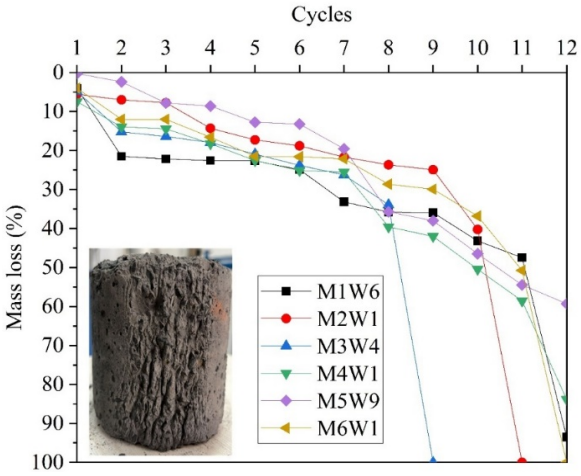

Figure 17. Mass loss of the specimen with number of wet-dry cycles

4. Conclusions

The current investigation focused on formulating a CLSM mixture incorporating industrial byproducts, including iron mine overburden combined with fly ash and cement as a binder. Through systematic experimental evaluation, it was found that all the CLSM mixtures demonstrated flow values exceeding 150 mm while maintaining bleeding below the 5% threshold. Further, the fresh density was found to range between 1226.80 and 1816.82 kg/m³, with hardened densities lower than that of the fresh density. The water absorption was found to vary from 1.19% to 28.24%, which is very close to the values reported by earlier researchers. The 28-day compressive strength ranged from 0.52 MPa to 4.28 MPa, meeting the suggested range of 0.3–8.3 MPa. Additionally, a few specimens exhibited a UCS value similar to stiff clay and a removability modulus of less than 1. Along with the strength comparable to clay, the developed CLSM shows good resistance to mass loss up to the 8th wet-dry cycle. Although all the developed CLSM can be used for different purposes, the mix with UCS similar to clay and a lower removability modulus could be employed to replace natural clay in geotechnical structures. Furthermore, due to some variability observed in the density and strength development of CLSM, further in-depth research is required to establish robust explanations.

6. References

[1]. Abelleira, A., Berke, N., & Pickering, D. (1998). Corrosion Activity of Steel in Cementitious Controlled Low-Strength Materials vs. That in Soil. In *The Design and Application of Controlled Low-Strength Materials (Flowable Fill)*. 100 Barr Harbor Drive, PO Box C700, West Conshohocken, PA 19428-2959: ASTM International.

[2]. ACI229R. (2013). *Report on Controlled Low Strength Materials (CLSM)*.

[3]. Adibee, N., Osanloo, M., & Rahmanpour, M. (2013). Adverse effects of coal mine waste dumps on the environment and their management. *Environmental Earth Sciences*, *70*(4), 1581–1592.

[4]. Alizadeh, V., Helwany, S., Ghorbanpoor, A., & Oliva, M. (2014). Rapid-Construction Technique for Bridge Abutments Using Controlled Low-Strength Materials. *Journal of Performance of Constructed Facilities*, *28*(1), 149–156.

[5]. Alizadeh, V., Helwany, S., Ghorbanpoor, A., & Sobolev, K. (2014). Design and application of controlled low strength materials as a structural fill. *Construction and Building Materials*, *53*, 425–431.

[6]. ASTM C39. (2023). *Standard Test Method for Compressive Strength of Cylindrical Concrete Specimens*.

[7]. ASTM C1610. (2021). *Standard Test Method for Static Segregation of Self-Consolidating Concrete Using Column Technique*. West Conshohocken: ASTM International.

[8]. ASTM D559. (2023). *Standard Test Methods for Wetting and Drying Compacted Soil-Cement Mixtures*. ASTM.

[9]. ASTM D854. (2023). *Standard Test Methods for Specific Gravity of Soil Solids by the Water Displacement Method*.

[10]. ASTM D2487-17. (2025). *Standard Practice for Classification of Soils for Engineering Purposes (Unified Soil Classification System)*. West Conshohocken, PA: ASTM International.

[11]. ASTM D6023. (2016). *Standard Test Method for Density (Unit Weight), Yield, Cement Content, and Air Content (Gravimetric) of Controlled Low-Strength Material (CLSM)*.

[12]. ASTM D6103. (2021). *Standard Test Method for Flow Consistency of Controlled Low Strength Material (CLSM)*. West Conshohocken: ASTM International.

[13]. ASTM D6913. (2017). *Standard Test Methods for Particle-Size Distribution (Gradation) of Soils Using Sieve Analysis*.

[14]. Chen, T., Yuan, N., Wang, S., Hao, X., Zhang, X., Wang, D., & Yang, X. (2022). The Effect of Bottom Ash Ball-Milling Time on Properties of Controlled Low-Strength Material Using Multi-Component Coal-Based Solid Wastes. *Sustainability (Switzerland)*, *14*(16). https://doi.org/10.3390/su14169949

[15]. Chi, M., & Huang, R. (2013). Binding mechanism and properties of alkali-activated fly ash/slag mortars. *Construction and Building Materials*, *40*, 291–298.

[16]. Chittoori, B., Puppala, A. J., & Raavi, A. (2014). Strength and Stiffness Characterization of Controlled Low-Strength Material Using Native High-Plasticity Clay. *Journal of Materials in Civil Engineering*, *26*(6).

[17]. Collins, F., & Sanjayan, J. G. (1999). Effects of ultra-fine materials on workability and strength of concrete containing alkali-activated slag as the binder. *Cement and Concrete Research*, *29*(3), 459–462.

[18]. Das, S. K., Mahamaya, M., & Reddy, K. R. (2020). Coal mine overburden soft shale as a controlled low strength material. *International Journal of Mining, Reclamation and Environment*, *34*(10), 725–747.

[19]. Das, S. K., & Yudhbir. (2005). Geotechnical Characterization of Some Indian Fly Ashes. *Journal of Materials in Civil Engineering*, *17*(5), 544–552.

[20]. Do, T. M., Kang, G.-O., Go, G.-H., & Kim, Y.-S. (2019). Evaluation of Coal Ash–Based CLSM Made

with Cementless Binder as a Thermal Grout for Borehole Heat Exchangers. *Journal of Materials in Civil Engineering*, *31*(6).

[21]. Dockter, B. (1998). Comparison of Dry Scrubber and Class C Fly Ash in Controlled Low-Strength Material (CLSM) Applications. In *The Design and Application of Controlled Low-Strength Materials (Flowable Fill)* (pp. 13-13–14). 100 Barr Harbor Drive, PO Box C700, West Conshohocken, PA 19428-2959: ASTM International.

[22]. Dutta, M., Khare, P., Chakravarty, S., Saikia, D., & Saikia, B. K. (2018). Physico-chemical and elemental investigation of aqueous leaching of high sulfur coal and mine overburden from Ledo coalfield of Northeast India. *International Journal of Coal Science & Technology*, *5*(3), 265–281.

[23]. Gabr, M. A., & Bowders, J. J. (2000). *Controlled low-strength material using fly ash and AMD sludge*. *Journal of Hazardous Materials* (Vol. 76). Retrieved from www.elsevier.nlrlocaterjhazmat

[24]. Gunathunga, S. U., Gagen, E. J., Evans, P. N., Erskine, P. D., & Southam, G. (2023). Anthropedogenesis in coal mine overburden; the need for a comprehensive, fundamental biogeochemical approach. *Science of The Total Environment*, *892*, 164515.

[25]. Gupta, A. K., & Paul, B. (2015). A review on utilisation of coal mine overburden dump waste as underground mine filling material: a sustainable approach of mining. *International Journal of Mining and Mineral Engineering*, *6*(2), 172.

[26]. Gupta, T., Mahamaya, M., & Alam, S. (2025). Development and Characterization of CLSM Using Mill Reject and Fly Ash: An Alternate Geo-Material. *Indian Geotechnical Journal*. https://doi.org/10.1007/s40098-025-01392-3

[27]. Han, J., Jo, Y., Kim, Y., & Kim, B. (2023). Development of High-Performance Fly-Ash-Based Controlled Low-Strength Materials for Backfilling in Metropolitan Cities. *Applied Sciences (Switzerland)*, *13*(16). https://doi.org/10.3390/app13169377

[28]. Horiguchi, T., Fujita, R., & Shimura, K. (2011). Applicability of Controlled Low-Strength Materials with Incinerated Sewage Sludge Ash and Crushed-Stone Powder. *Journal of Materials in Civil Engineering*, *23*(6), 767–771.

[29]. Islam, N., Rabha, S., Subramanyam, K. S. V., & Saikia, B. K. (2021). Geochemistry and mineralogy of coal mine overburden (waste): A study towards their environmental implications. *Chemosphere*, *274*, 129736.

[30]. Ismail, I., Bernal, S. A., Provis, J. L., San Nicolas, R., Brice, D. G., Kilcullen, A. R., Hamdan, S., & van Deventer, J. S. J. (2013). Influence of fly ash on the water and chloride permeability of alkali-activated slag mortars and concretes. *Construction and Building Materials*, *48*, 1187–1201.

[31]. Katz, A., & Kovler, K. (2004). Utilization of industrial by-products for the production of controlled low strength materials (CLSM). *Waste Management*, *24*(5), 501–512.

[32]. Kong, X., Wang, G., Rong, S., Liang, Y., Liu, M., & Zhang, Y. (2023). Utilization of Fly Ash and Red Mud in Soil-Based Controlled Low Strength Materials. *Coatings*, *13*(5).

[33]. Kuo, W. Ten, & Gao, Z. C. (2018). Engineering properties of controlled low-strength materials containing bottom ash of municipal solid waste incinerator and water filter silt. *Applied Sciences (Switzerland)*, *8*(8).

[34]. Le, D. H., & Nguyen, K. H. (2016). An assessment of eco-friendly controlled low-strength material. In *Procedia Engineering* (Vol. 142, pp. 260–267). Elsevier Ltd.

[35]. Lee, S. Y., Yoon, H. H., Son, M., Kong, J. Y., & Jung, H. S. (2018). Controlled Low Strength Material for Emergency Restoration Using Bottom Ash and Gypsum. *Journal of the Korean Geosynthetics Society*, *17*(2), 19–31.

[36]. Li, Y., Liu, S., & Guan, X. (2021). Multitechnique investigation of concrete with coal gangue. *Construction and Building Materials*, *301*, 124114.

[37]. Ling, T. C., Kaliyavaradhan, S. K., & Poon, C. S. (2018, January 15). Global perspective on application of controlled low-strength material (CLSM) for trench backfilling – An overview. *Construction and Building Materials*. Elsevier Ltd.

[38]. Mahamaya, M., Alam, S., & Kumar Das, S. (2024). Development and characterization of alkali activated controlled low strength material using mining waste. *Construction and Building Materials*, *452*, 138928.

[39]. Mahamaya, M., & Das, S. K. (2017). Characterization of mine overburden and fly ash as a stabilized pavement material. *Particulate Science and Technology*, *35*(6), 660–666.

[40]. Mahamaya, M., & Das, S. K. (2020). Characterization of ferrochrome slag as a controlled low-strength structural fill material. *International Journal of Geotechnical Engineering*, *14*(3), 312–321.

[41]. Mahamaya, M., Jain, S., Das, S. K., & Paul, R. (2023). Engineering Properties of Cementless Alkali Activated CLSM Using Ferrochrome Slag. *Journal of Materials in Civil Engineering*, *35*(3).

[42]. Mahima Kumar, M., Senthilvadivu, R., Brahmaji Rao, J. S., Neelamegam, M., Ashok Kumar, G. V. S., Kumar, R., & Jena, H. (2020). Characterization of fly ash by ED-XRF and INAA for the synthesis of low silica zeolites. *Journal of Radioanalytical and Nuclear*

Chemistry, *325*(3), 941–947. https://doi.org/10.1007/s10967-020-07243-0

[43]. Mitchell, J. K., & Houston, W. N. (1969). Causes of Clay Sensitivity. *Journal of the Soil Mechanics and Foundations Division*, *95*(3), 845–871. https://doi.org/10.1061/JSFEAQ.0001288

[44]. Mohapatra, M., & Anand, S. (2007). Studies on sorption of Cd(II) on Tata chromite mine overburden. *Journal of Hazardous Materials*, *148*(3), 553–559.

[45]. Okuyucu, O., Jayawickrama, P., & Senadheera, S. (2019). Mechanical Properties of Steel Fiber–Reinforced Self-Consolidating Controlled Low-Strength Material for Pavement Base Layers. *Journal of Materials in Civil Engineering*, *31*(9).

[46]. Poulsen, B., Khanal, M., Rao, A. M., Adhikary, D., & Balusu, R. (2014). Mine Overburden Dump Failure: A Case Study. *Geotechnical and Geological Engineering*, *32*(2), 297–309.

[47]. Raghavendra, T., & Udayashankar, B. C. (2014). Flow and Strength Characteristics of CLSM Using Ground Granulated Blast Furnace Slag. *Journal of Materials in Civil Engineering*, *26*(9).

[48]. Raghavendra, T., & Udayashankar, B. C. (2015). Engineering properties of controlled low strength materials using flyash and waste gypsum wall boards. *Construction and Building Materials*, *101*, 548–557.

[49]. Singh, K. N., & Narzary, D. (2021). Geochemical characterization of mine overburden strata for strategic overburden-spoil management in an opencast coal mine. *Environmental Challenges*, *3*, 100060.

[50]. Wagner, J.-F. (2013). Mechanical Properties of Clays and Clay Minerals (pp. 347–381).

[51]. Williams, J. A., Parmar, D., & Conroy, M. W. (1994). Controlled backfill optimization to achieve high ampacities on transmission cables. *IEEE Transactions on Power Delivery*, *9*(1), 544–552.

[52]. Won, J. P., Lee, Y. S., Park, C. G., & Park, H. G. (2004). Durability characteristics of controlled low-strength materials containing recycled bottom ash. *Magazine of Concrete Research*, *56*(7), 429–436.

[53]. Wu, H., Huang, B., Shu, X., & Yin, J. (2016). Utilization of solid wastes/byproducts from paper mills in Controlled Low Strength Material (CLSM). *Construction and Building Materials*, *118*, 155–163.

[54]. Yan, D. Y. S., Tang, I. Y., & Lo, I. M. C. (2014). Development of controlled low-strength material derived from beneficial reuse of bottom ash and sediment for green construction. *Construction and Building Materials*, *64*, 201–207. https://doi.org/10.1016/j.conbuildmat.2014.04.087

[55]. Yuan, B., Yuan, S., Straub, C., & Chen, W. (2020). Activation of Binary Binder Containing Fly Ash and Portland Cement Using Red Mud as Alkali Source and Its Application in Controlled Low-Strength Materials. *Journal of Materials in Civil Engineering*, *32*(2).

[56]. Zhang, L., Wang, Z., Cao, J., Zeng, X., Tian, F., Xin, F., & Huang, J. (2025). Influence mechanisms and control effects of overburden on rock slope stability: case study in Yanqianshan iron mine, China. *Bulletin of Engineering Geology and the Environment*, *84*(4), 197.

[57]. Zhang, X., & Han, J. (2000). The effect of ultra-fine admixture on the rheological property of cement paste. *Cement and Concrete Research*, *30*(5), 827–830.

نشریه مهندسی معدن و محیط زیست
نشانی نشریه: www.jme.shahroodut.ac.ir
انجمن مهندسی معدن ایران
دانشگاه صنعتی شاهرود

مقاومت و دوام CLSM مبتنی بر سیمان که با استفاده از روباره معدن آهن توسعه داده شده است

تولیکا گوپتا[1]، ماهاساکتی ماهامایا[1] و شمشاد علم[2*]

۱. گروه مهندسی عمران، دانشکده مهندسی، دانشگاه OP Jindal، رایگر، هند.
۲. گروه مهندسی عمران و معماری، دانشکده مهندسی و علوم کامپیوتر، دانشگاه جزان، جزان، عربستان سعودی

اطلاعات مقاله

تاریخ ارسال: ۲۰۲۵/۰۸/۱۹
تاریخ داوری: ۲۰۲۵/۰۹/۲۶
تاریخ پذیرش: ۲۰۲۵/۱۱/۱۵

DOI:10.22044/jme.2025.16705.3277

کلمات کلیدی

جریان پذیری
خونریزی
قدرت
ماندگاری

چکیده

تخلیه زباله‌های معدنی مناطق وسیعی از زمین را اشغال می‌کند و خطرات زیست محیطی از جمله شسته شدن فلزات سنگین، آلودگی گرد و غبار و خرابی شیب‌ها را به همراه دارد. سربار معدن آهن (MO)، محصول جانبی معدن آهن، این مسائل را در هنگام تخلیه تشدید می‌کند. برای مقابله با چالش‌های ذخیره‌سازی MO، با خاکستر بادی و سیمان ترکیب شد تا مواد کنترل‌شده با استحکام پایین (CLSM) تولید شود. در ابتدا مواد اولیه از نظر خواص فیزیکی، شیمیایی و کانی شناسی مورد بررسی قرار گرفتند. متعاقباً، ۲۴ مخلوط مختلف CLSM با نسبت سیمان، خاکستر بادی، MO و آب به اتصال دهنده تهیه شد. مخلوط‌های تازه برای روان‌پذیری، خونریزی و چگالی تازه مورد آزمایش قرار گرفتند، در حالی که خواص سخت‌شده، از جمله چگالی، مقاومت فشاری محدود (UCS)، و دوام نیز مورد ارزیابی قرار گرفتند. نتایج نشان داد که همه مخلوط‌های CLSM بسیار روان بودند، با قطر جریان بیش از ۱۵۰ میلی‌متر، و برخی از آنها رفتار خود تراز نشان دادند. مقاومت فشاری ۲۸ روزه از ۰.۵۲ مگاپاسکال تا ۴.۲۸ مگاپاسکال متغیر بود و چند مخلوط به اندازه کافی برای حفاری دستی نرم بودند. آزمایش‌های دوام نشان داد که تقریباً ۶۰٪ از جرم پس از هشت چرخه مرطوب-خشک دست نخورده باقی مانده است که مقاومت خوبی در برابر فرسایش نشان می‌دهد. این مطالعه پتانسیل استفاده از ضایعات معدنی در مصالح ساختمانی پایدار را برجسته می‌کند.

نویسنده مسئول مکاتبات: shalam@jazanu.edu.sa (ش. علم)